ACS OMEGA

http://pubs.acs.org/journal/acsodf

Article

Biofriendly Waste Shell Powders/Polylactic Acid Composites for Antibacterial Engineering Applications

Yuansen Liu,[#] Jiajun Guo,[#] Xinqing Zheng, Kexin Tang, Ling Lin,[*] and Min Nie[*]

Cite This: *ACS Omega* 2022, 7, 36672−36678

Read Online

ACCESS | Metrics & More | Article Recommendations

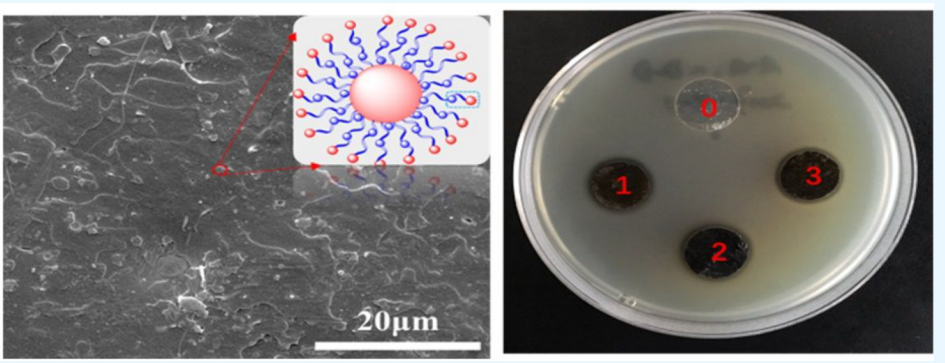

ABSTRACT: With the rapid progress of agriculture and aquaculture, waste shells are harming the environment because of large production, and highly valued recycling is now holding more attention. However, there are still no good ways for simultaneously solving the poor mechanical and antibacterial performance during the recycling process. In this work, antibacterial shell-grafting-Ag powders/polylactic acid (shell-g-Ag/PLA) biocompatible composites, with comparable mechanical properties to industrial polymer counterparts, were prepared via the in situ reduction of Ag ions on surfaces of polydopamine-modified shell powders. The introduction of Ag particles increases the compatibility on the interface and endows the composites with antibacterial performance by inheriting the prominent characteristic from Ag. Without scarifying the mechanical properties by improving the crystallinity and interface, the loaded Ag particles in the composites endowed the composites with valorized antibacterial performance, evidenced by a bacterial inhibition width from 0 to ∼3.29 mm. The biofriendly composites, together with comparable mechanical properties to industrial PLA products, can serve as a sustainable material to be applied in the field of disposable packaging.

INTRODUCTION

Since the worldwide encouragement of green economy and low-carbon life, there is a growing trend toward the application of natural sources from disposable use to a closed loop of produce, recycle, and reuse.[1−3] Shellfish products, serving as an important component of the food industry, are typically disposable where the meat is enjoyed and the shells are ruthlessly discarded.[4] Up to now, there are about 10 million tons of waste shells annually dumped in soils or abandoned along the coastline, seriously burdening cities and the environment.[5] In fact, the abandoned shells are misplaced treasures because the main components of them are an industrial reinforcing additive: calcium carbonate ($CaCO_3$).[6] It is envisioned that the waste shells can also be reasonably applied for strengthening polymers or construction materials, the recycling of which definitely not only decreases the necessary cost of industrial products but also relieves environmental issues. Thereby, it is of great meaning to build the subsequent recycle and reuse line of shellfish products.

When adding fillers into polymer matrix, the aim is to strengthen or, at least, not sacrifice the mechanical properties. An excellent interface in a composite system is a prerequisite for valuing the recycling of waste shells.[7,8] Waste shell powders (WSPs) have been previously introduced into some polymers like acrylonitrile butadiene styrene (ABS),[9] polypropylene (PP),[10] polyethylene (PE),[11] etc. The interfacial interactions between polymers and WSPs are too weak to cover the demand of reinforcing polymers, with a post-treatment on the surface of WSPs or the addition of compatibilizers needed to improve the interface.[10,12] However, the addition of foreign additives such as maleic anhydride grafting polymers and

Received: July 28, 2022
Accepted: October 3, 2022
Published: October 7, 2022

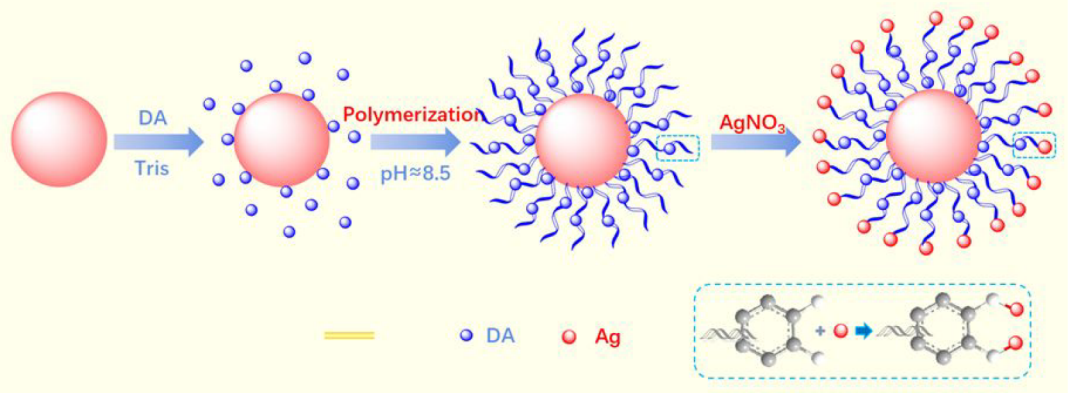

Figure 1. Schematic of Ag-functionalized shell powders.

cetyltrimethylammonium bromide can unexpectedly threaten potential toxicity, limiting the scope of application in biomedicine, the food industry, and some others. Thus, it is still a big challenge to dig out proper compatibilizing techniques while not affecting the biocompatibility.

Grafting a biofriendly interlayer into the composites that improves the interface can be the solution to the above questions. Currently, there are some biorelated materials available for surface modification including hydroxyapatite (HA),[13] graphene oxide (GO),[14] polydopamine (PDA),[15] and so on. It is reported that sharp and rough interfaces between the coating layer and the polymers can be formed by a strong interfacial interaction, improving mechanical robustness.[16] Among these availabilities, the surface coating of PDA is the ideal choice due to the gentle reaction condition and the strong adhesion of PDAs to substrates.[17] Once introduced as an interfacial compatibilizer, PDAs have been witnessed great energy in bridging polymer and fillers, metal coordination, and various chemical reactions owing to the functional groups existing on the PDAs.[18] It is reported that the reduction reaction of Ag ions into Ag particles can be achieved via the chelation with functional groups from PDA, which further increases the interfacial locking and endows the composites with antibacterial performance by inheriting a superior characteristic from Ag.[19−21] Thus, a dopamine coating technique and subsequent Ag particle loading are promising for valuable recycling of WSPs as biofriendly engineering composites.

In this work, antibacterial PLA/shell biocomposites were prepared for the purpose of highly valued recycling and reuse of waste shells. The dopamine surface coating technique and subsequent in situ reduction of Ag+ into Ag particles were combined to load Ag particles onto the shell powders, where there was a flexible content of reduced Ag particles by controlling the self-polymerization time of dopamine. Then, shell-g-Ag powders were introduced into PLA matrix. The crystallization, interface, and mechanical and antibacterial performance were all systematically investigated. As a result, the loading of Ag significantly compatibilized the interface between PLA and shell powders and endowed the composites with comparable mechanical performance to neat PLA and valorized antibacterial performance. Exactly different from the traditional recycling of waste shell powders, this work solves simultaneously the poor mechanical and antibacterial performance by utilizing Ag and PDA as interfacial compatibilizers, which is a totally new strategy toward highly valued recycling of waste shells.

EXPERIMENTAL SECTION

Materials. Polylactic acid (PLA, trade name: 4032D) with a weight-average molecular weight of 160 kg/mol was purchased from UNIC Technology Co., Ltd. (Suzhou, China). Waste shells were kindly provided by State Oceanic Administration No.3 Ocean Institute (Fujian, China) and then were ground into fine powders as mentioned in our previous work.[10] Dopamine hydrochloride was purchased from Aoduofuni Biological Technology Co. (Nanjing, China). Silver nitrate ($AgNO_3$) and tris(hydroxymethyl) aminomethane (Tris) were supplied by Chengdu Kelong Chemical Reagent Factory (Chengdu, China).

Sample Preparation. *Preparation of Ag-Functionalized Shell Powders.* Figure 1 illustrates the surface functionalization procedure of Ag-loading shell powders. Based on the dopamine surface coating technique, shell powders were first dispersed in 20 mg/mL dopamine hydrochloride solution, where the pH was treated to 8.5 using Tris-HCl buffer.[22] After t_1 hours stirring at room temperature, redundant additives were removed by repeated washing in distilled waters. Then, 5 mM $AgNO_3$ solution was added into the obtained PDA-coating shell powders, and then, the mixture was stirred at room temperature under magnetic stirring for 6 h. Finally, the resultant precipitants were cleaned with deionized water for several times to remove the free silver ions, and Ag-functionalized shell powders were obtained. To evaluate the role of PDA-coating layer on the loading content of Ag particles, t_1 was set as 0, 4, 6, and 8 h, respectively. The resultant powders were named as shell, shell-g-Ag1, shell-g-Ag2, and shell-g-Ag3, respectively.

Preparation of PLA/Shell Composites. To realize the value-added application of waste shell powders, shell and shell-g-Ag (8 h self-polymerization of dopamine) were both introduced into the PLA matrix. First, the shell powders were melt-blended with PLA granules using a twin-screw mixer (RM-200C, Harbin Hapro Electric Technology Co., Ltd., China) with a loading percent, screw rotation rate, processing temperature, and mixing time of 10%, 50 rpm, 180 °C, and 5 min, respectively. Then, the composites were injection-molded into standard specimens for tensile and impact testing.

Characterization. *Scanning Electron Microscopy (SEM) with Energy Dispersive X-ray Spectrometry.* Surface morphologies of shell powders and with Ag loading were both observed using an Inspect SEM instrument at 0.5 Torr and 20 kV, and the element constituents were obtained by energy dispersive X-ray spectrometry (EDS). The cross section

https://doi.org/10.1021/acsomega.2c04779
ACS Omega 2022, 7, 36672−36678

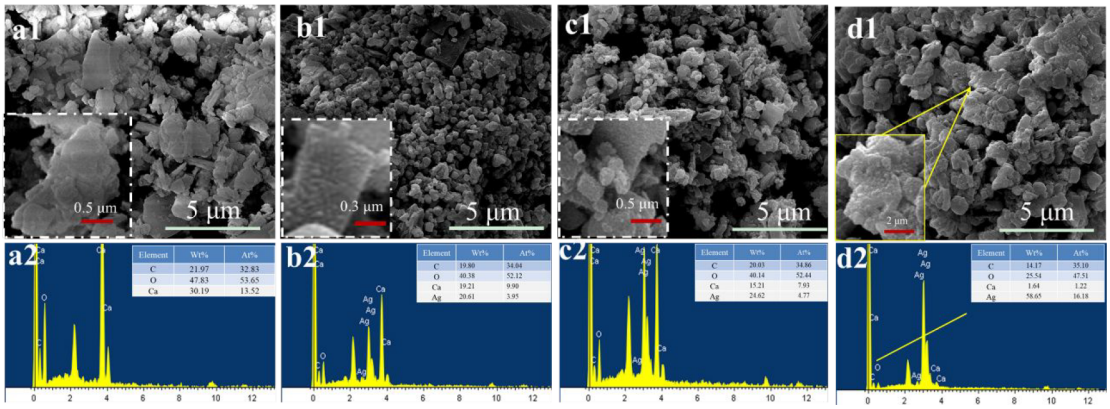

Figure 2. SEM photos of pristine shell powders (a1), shell powders grafted by Ag particles with different doping contents (b1−d1), and the corresponding EDS analysis (subscript 2), with the inset of the surface morphologies under Ag loading.

of PLA/shell composites was also observed. The specimens were quenched under liquid nitrogen, fractured, and then were all gold-sputtered.

X-ray Diffraction (XRD). XRD measurement was carried out using a DX-1000 diffractometer (Dandong Fangyuan Instrument Co.Ltd., China). The CuKa generator system was conducted at 40 kV and 25 mA. The range of scanning 2θ was 15−50°, with a scanning rate of 5 °/min.

Differential Scanning Calorimetry (DSC) Analysis. The crystallization behaviors of the samples were analyzed using a Q20 differential scanning calorimetry apparatus (TA, USA). Samples of ∼5−10 mg were heated from 40 to 200 °C at a heating rate of 10 °C/min under nitrogen atmosphere. The calculation of crystallinity takes into consideration the rearrangement of molecular chains adjacent to the ordered parts during the secondary heating, named as "cold crystallization". The practical crystallinity (χc) for the PLA blends was expressed as eq 1:

$$\chi_c(\%) = \frac{\Delta H_m - \Delta H_{cc}}{\Delta H_o} \times 100\% \quad (1)$$

where ΔH_m is the melt enthalpy around T_m, ΔH_{cc} is recrystallization enthalpy around T_{cc}, and ΔH_o is the enthalpy for 100% crystalline PLA (93.7 J/g).[23]

Mechanical Measurements. The dumbbell shaped specimens were tested on a universal testing machine (model RG L-10, Shenzhen Reger Instrument Co.) with a tensile rate of 50 mm/min according to GB/T 1040.2−2006. The strength at the fracture was recorded as axial tensile strength. The notched Izod impact toughness of the specimens with a V-notch of 2 mm depth was measured via an Izod machine XBJ-7.5/11 (Chang Chun Testing Machine Co.) according to GB/T1843−1996. The toughness was obtained by dividing the impact energy to cross-sectional area at the notch.

Antibacterial Performance Measurement. The antibacterial performance was evaluated by observing the diffusion width gap against *E. coli*.[24] The bacteria were cultivated in sterilized Luria−Bertani (LB) broth at 37 °C for 16 h, and the fresh media was put onto agar plate. Then, the sample was compression-molded into circular shapes with a diameter of ∼14 mm and were put into inoculated agar plates and cultivated under visible light irradiation at 37 °C for 24 h. The antibacterial performance was evaluated based on the area of the inhibition width.

RESULT AND DISCUSSION

Functionalization of Shell Powders with Ag Nanoparticles. The surface morphologies and constituents of WSPs were characterized using SEM and EDS analysis. As shown in Figure 2a1,a2, the surfaces of pristine shell powders were smooth, and many small shell particles aggregated into large ones. EDS analysis proved the constituent of Ca, C, and O elements, which illustrated the constituents of natural shells. However, the size of shell powders was obviously small after a two-step loading of Ag particles in Figure 2b1 and the inset. The decreased particle size here can be attributed to the electrostatic repulsion between adjacent PDA layer coating on shell powders during the dopamine self-polymerization, thus decreasing the interfacial tension and the particle size. Furthermore, the atom loading content of Ag can be quantified as 3.95% from EDS analysis (Figure 2b2). It is well-documented that the PDA layers can recruit the free Ag+ anchored onto the surface, and then, the reduction reaction of Ag ions into Ag nanoparticles can proceed through the chelation between Ag+ and catechol groups of PDA.[25] It can be further deduced that increasing PDAs coated on the base would also increase the loading content of Ag nanoparticles. By manipulating the reaction time of dopamine from 4 to 8 h, Ag-loading contents were significantly improved from 3.95 to 16.18% (Figure 2b1−d1). Accordingly, the average particle size was also improved due to the increased loading of Ag particles. At last, Ag particles loaded on shell powders were clearly shown in the inset of Figure 2a1−d1. The Ag particles loaded on shell powders obviously led to a rough surface of shell powders, which benefits locking the interface from the enlarged interfacial areas and interactions.

The crystallization information on shell and shell-g-Ag powders was characterized using XRD analysis. Figure 3 displayed the XRD patterns as a function of Ag-loading content. After Ag grafting, the characteristic reflection at ∼19° appeared. This can be originated from partial transformation of shell powders into $Ca(OH)_2$ during the surface modification. A similar phenomenon was also investigated in other research.[26] Moreover, the diffraction peaks located at 23.1, 29.4, 31.4, 35.9, 39.4, 43.2, 47.5, and 48.5° correspond to (012), (104), (006), (110), (113), (202), (018), and (116) reflections of the hexagonal phase calcite (JCPDS 88−1807),[27] while the peak at 38.1° is a characteristic (111) reflection of Ag particles.[19] It is safely concluded from the XRD patterns that free Ag^+ ions from the $AgNO_3$ solution were successfully transformed into

https://doi.org/10.1021/acsomega.2c04779
ACS Omega 2022, 7, 36672−36678

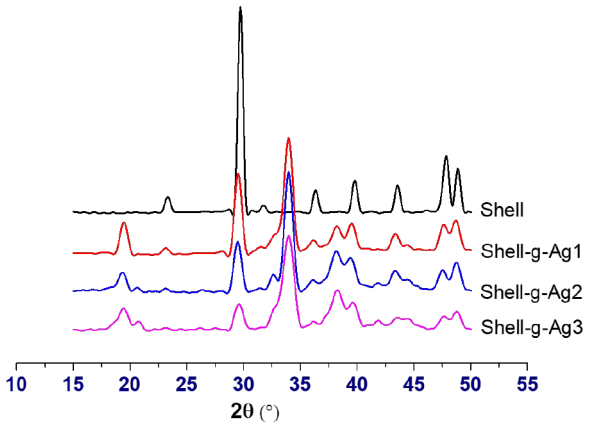

Figure 3. XRD patterns of shell powders before and after Ag grafting.

the Ag nanoparticle. Here, by manipulating the self-polymerization time of dopamine as 4, 6, and 8 h, the loading content of Ag was significantly improved as explained. Correspondingly, the characteristic reflection at 38.1° was also enhanced as a function of the loading content of Ag particles.

Structure and Mechanical Performance of PLA/Shell Composites. The main components of shell powder have been proved to be $CaCO_3$. The outstanding characteristics of low cost, easy availability, and high modulus determine the worldwide use of $CaCO_3$ for reinforcing polymers or construction materials in industrial applications. However, it is well-accepted that direct blending of inorganic fillers and polymers can unsurprisingly cause weak interfacial bonding from poor compatibility between the polymers and fillers.[28] As shown in Figure 4a, the red circle represented the cavities formed from the shedding of loading particles during the fracturing progress, which was also the symbol of poor interfacial compatibility between the two components. It is well-known that stress concentrated preferentially in the place with defects or weak interactions.[29] Then, the crazing is keen on propagating at the weak points of the interface between shell powders and PLA matrix, leading to the easy fracture and shedding of loading particles at the interface. Therefore, surface modification of shell powders to build the interface is necessary for the valorized application as reinforcing additives. Considering the largest amount of Ag particles loaded on shell powders, the self-polymerization time of dopamine was set as 8 h (shell-g-Ag3). As shown in Figure 4b, the shell-g-Ag3 powders with 16.18% Ag firmly embedded on the PLA matrix without any cavities, successfully proving the enhanced interfacial compatibility. The complexation between polymers and functional groups from PDA layers, the rough interface brought by loading of Ag, together with the decrescent particle size, may be the reasons underlying the improved interface. It is reported that catechol groups can complex with polar groups from PLA chains and build in contact with strong interactions.[30] The surface roughness from introduction of Ag enables more contact area to locking the interface. As a result, the strong interaction compatibilized the interface and enabled more stress exerted on the reinforcing additives, thus decreasing the danger of fracturing at the interface. In addition, it was reported recently that there are more interfacial areas and interactions as the loading particles decrease in particle size and simultaneously the loading content is not changed, which can further reinforce the total interface interactions.[31] The size effect also explains the common use of nanosized fillers in polymer composites.

In addition to the interface, the understanding of crystallization is also crucial for PLA-related products. There are three characteristic points including glass transition temperature (T_g), cold crystallization temperature (T_{cc}), and melting temperature (T_m). As shown in Figure 5a, T_g and T_m were not significantly changed, representing that the molecular chain mobility was influenced little. However, T_{cc} and the melting range of cold crystallization were obviously different under shell/shell-g-Ag incorporation. Compared to neat PLA, the T_{cc} of PLA/shell composites shifted to lower temperatures. Additionally, the melting range of cold crystallization simultaneously decreased, indicating that introduction of shell powders perfected the crystals during crystallization and reduced the thermal energy for aligning the imperfect molecular chains into the lattice in the secondary heating. As was shown in Figure 5b, the crystallinity of cold crystallization (χ_{cc}) significantly decreased from 65% for PLA to 33% for PLA/SP and 42% for PLA/shell-g-Ag3. It is widely accepted that the molecular mobility of PLA is very poor and there is a large amount of imperfect molecular chains arranged into the lattice under cooling. During the secondary heating, this part of molecular chains will rearrange and crystallize in lower thermodynamic potential, named as cold crystallization. The introduction of foreign additives can serve as a heterogeneous nucleating agent and benefit the crystallization of PLA during the sample preparation, decreasing the percent of cold

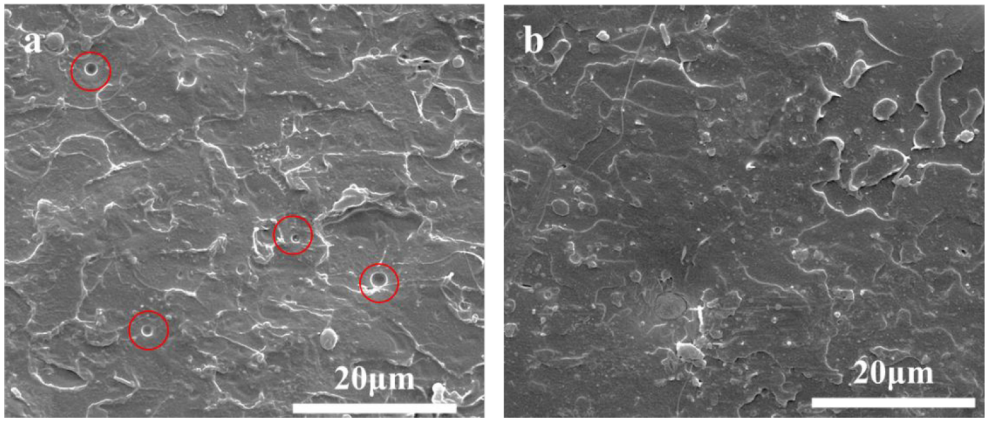

Figure 4. SEM photos of PLA/shell composites: PLA/shell (a); PLA/shell-g-Ag3 (b).

https://doi.org/10.1021/acsomega.2c04779
ACS Omega 2022, 7, 36672−36678

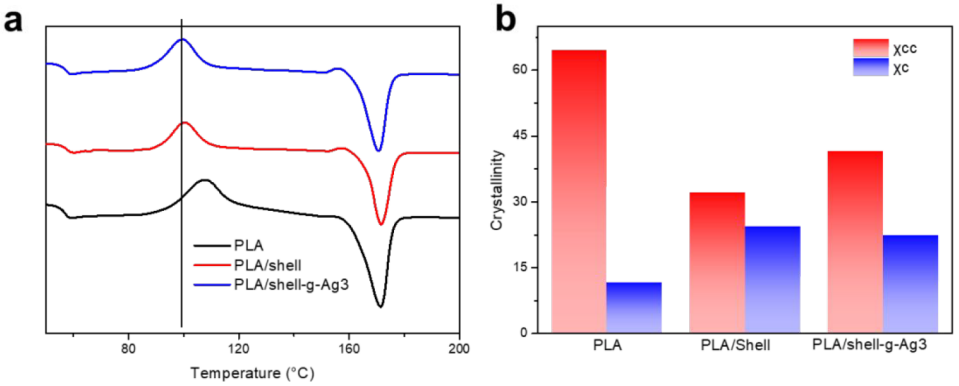

Figure 5. DSC curves (a) and calculated crystallinity (b) of PLA/shell composites.

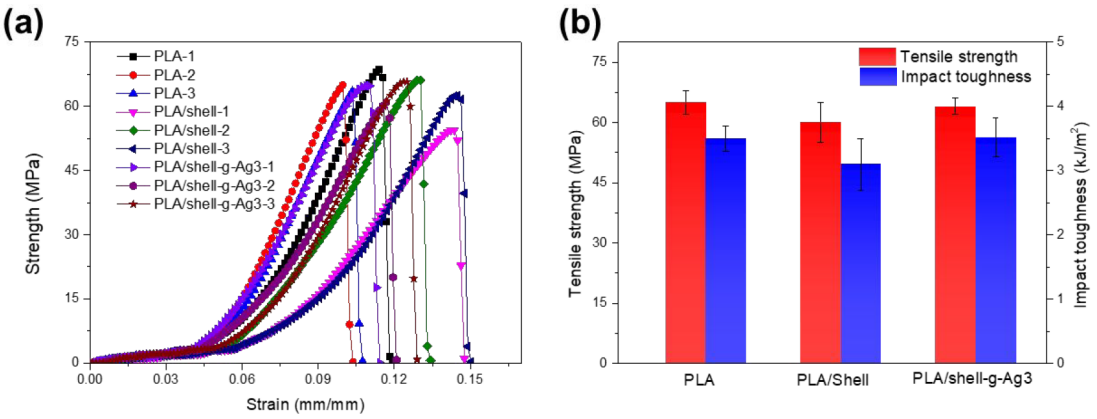

Figure 6. Uniaxial tensile curves (a) and mechanical strength (b) of PLA/shell composites.

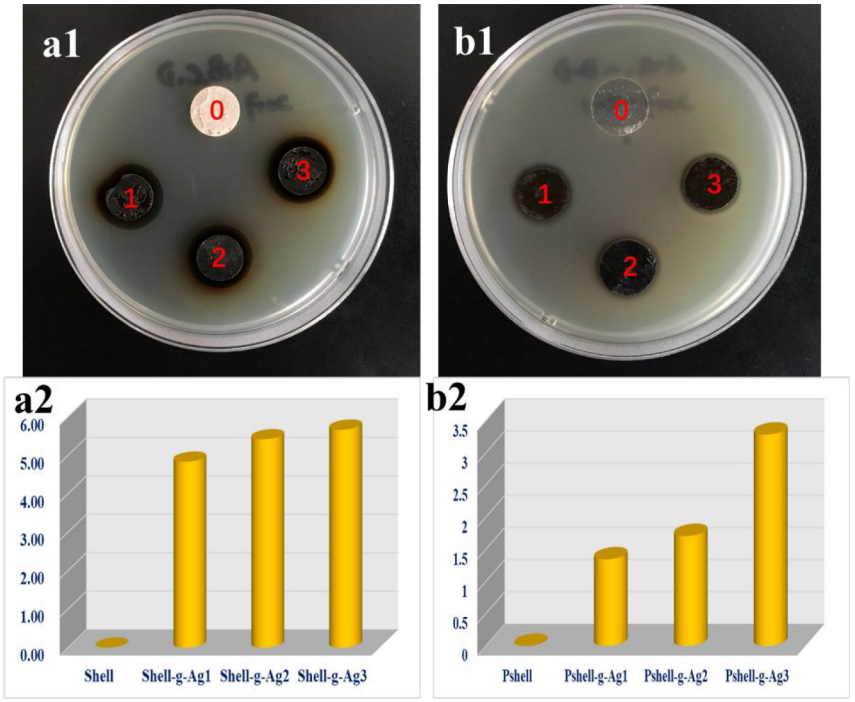

Figure 7. Diffusion inhibition zones of shell (a1) and PLA/shell composites (b1) against *E. coli* and the corresponding sizes of the inhibition zones (a2,b2).

crystallization during secondary heating. Thus, PLA/shell composites showed a decreased χ_{cc} as compared to neat PLA. However, the eccentric increase in χ_{cc} after Ag loading on shell powders may originate from the decreased numbers of shell particles and reduced nucleation sites for heterogeneous nucleation. Finally, the practical χ_c of the as-prepared sample

https://doi.org/10.1021/acsomega.2c04779
ACS Omega 2022, 7, 36672−36678

can be obtained by the difference between χ_c and χ_{cc}. By calculating the crystallinity using eq 1, the practical crystallinity was significantly improved from 11% for neat PLA to 25% for PLA/shell and 21% for PLA/shell-g-Ag3 composites, showing the opposite trend to χ_{cc} due to the different nucleation abilities of foreign additives as explained above.

Figure 6a,b provided the tensile curves and the impact strength of PLA/shell composites. The tensile and impact strength of neat PLA reached ∼65 MPa and 3.5 kJ/m^2, respectively. However, there were a large descent in mechanical properties after incorporating shell powders, with a decrease of ∼10% in tensile strength and ∼9% in impact toughness. It was due to the poor interface that the crazing propagated preferentially at the weak point of interface, and deteriorated properties were obtained as explained.[10] By surface loading of Ag particles and PDA layers, the mechanical properties almost reached the same level as neat PLA due to the improved interfaces and crystallinity. The value-added application of shell powders and surface modification for an improved interface can reduce largely the cost of industrial PLA products and relieve the serious environmental issues brought by excessive use of white plastics.

At last, another tough issue brought by the introduction of the biomass matrix is the sign of mustiness in the course of time, deteriorating the mechanical performance and threatening health problems. Therefore, the disk diffusion method was applied necessarily for deep understanding of the long-term applicability of PLA/shell composites. Before the test, all the samples were compression-molded into circular shapes with an equal size of ∼14 mm, and then, the antibacterial performance was recorded. Specifically, the pristine shell powders were compression-loaded on the surface of paper. As shown in the region marked as 0 in Figure 7a1,b1, bacteria can easily reproduce on surface of shell and PLA/shell composites with almost no inhibition zones. It proves that PLA or shell cannot effectively inhibit the bacteria proliferation, as evidenced by the routine experience of the moss on waste shells. However, it is not the case for surface modification on a shell as a pristine shell behaves. By inheriting the antibacterial advantages of Ag, the functionalized shell powders and the composites can both wipe out the bacteria in vicinity of the circular sample. As shown in the regions marked as 1, 2, and 3 in Figure 7a1,b1, the proliferous bacteria cannot propagate around shell-g-Ag or PLA/shell-g-Ag3 composites, with impressive circular inhibition zones. More importantly, the width gap of circular inhibition zones represented the antibacterial ability and here kept a linear relationship to the Ag-loading content. As the loading content of Ag varied from 3.95 to 16.18%, the inhibition width of shell-g-Ag and PLA/shell-g-Ag composites increased significantly from ∼4.84 and ∼1.35 mm to ∼5.67 and ∼3.29 mm, respectively. It can be deduced that this functionalized method owns a broad prospect toward the long-term application of PLA/shell composites as disposable packaging.[32]

CONCLUSION

In this work, we put forward a facile strategy to endow the waste seashell/PLA composites with simultaneous mechanical robustness and high antibacterial performance. The PDA layer formed by self-polymerization of dopamine can recruit free Ag ions and reduce Ag+ to Ag particles onto the surface via the chelation between Ag+ and the catechol group. By operating on a self-polymerization time of dopamine from 4 to 8 h, the loading of Ag particles was further controlled from 3.95 to 16.18% on the surfaces of shell powders, which significantly improved the interface and crystallinity. Further, by inheriting the antibacterial properties from Ag particles, the composites showed a large bacterial inhibition zone of 3.29 mm. The mechanical robustness and antibacterial properties of the composites can largely reduce the cost of industrial PLA products, thus opening the door toward the highly valued reuse of waste shells.

AUTHOR INFORMATION

Corresponding Authors

Min Nie − *State Key Laboratory of Polymer Materials Engineering, Polymer Research Institute of Sichuan University, Chengdu 610065, China*; orcid.org/0000-0001-8386-7547; Phone: +86-28-85405133; Email: poly.nie@gmail.com; Fax: +86-28-85402465

Ling Lin − *Technology Innovation Center for Exploitation of Marine Biological Resources, Third Institute of Oceanography, Ministry of Natural Resources, Xiamen 361005, China*; Email: linling@tio.org.cn

Authors

Yuansen Liu − *Technology Innovation Center for Exploitation of Marine Biological Resources, Third Institute of Oceanography, Ministry of Natural Resources, Xiamen 361005, China*

Jiajun Guo − *State Key Laboratory of Polymer Materials Engineering, Polymer Research Institute of Sichuan University, Chengdu 610065, China*

Xinqing Zheng − *Technology Innovation Center for Exploitation of Marine Biological Resources, Third Institute of Oceanography, Ministry of Natural Resources, Xiamen 361005, China*

Kexin Tang − *Technology Innovation Center for Exploitation of Marine Biological Resources, Third Institute of Oceanography, Ministry of Natural Resources, Xiamen 361005, China*

Complete contact information is available at: https://pubs.acs.org/10.1021/acsomega.2c04779

Author Contributions

#Y.L. and J.G. contributed equally to this work.

Notes

The authors declare no competing financial interest.

ACKNOWLEDGMENTS

This work is funded by the Scientific Research Foundation of Third Institute of Oceanography, MNR (2017028), the State Key Laboratory of Polymer Materials Engineering (sklpme2019-2-11/sklpme2022-4-02), the Science and Technology Planning Project of Fujian Province, China (2021Y0065), and the Xiamen Ocean Research and Development Institute (KFY202203).

REFERENCES

(1) Browne, M. A.; Crump, P.; Niven, S. J.; Teuten, E.; Tonkin, A.; Galloway, T.; Thompson, R. Accumulation of microplastic on shorelines woldwide: sources and sinks. *Environ. Sci. Technol.* **2011**, *45*, 9175−9179.

(2) Schneider, M.; Romer, M.; Tschudin, M.; Bolio, H. Sustainable cement production—present and future. *Cem. Concr. Res.* **2011**, *41*, 642−650.

(3) Damtoft, J. S.; Lukasik, J.; Herfort, D.; Sorrentino, D.; Gartner, E. M. Sustainable development and climate change initiatives. *Cem. Concr. Res.* **2008**, *38*, 115−127.
(4) Zhang, Y.; Chen, D.; Liang, Y.; Qu, K.; Lu, K.; Chen, S.; Kong, M. Study on engineering properties of foam concrete containing waste seashell. *Constr. Build. Mater.* **2020**, *260*, 119896.
(5) Mo, K. H.; Alengaram, U. J.; Jumaat, M. Z.; Lee, S. C.; Goh, W. I.; Yuen, C. W. Recycling of seashell waste in concrete: A review. *Constr. Build. Mater.* **2018**, *162*, 751−764.
(6) Xie, Y.; Han, R.; Li, L. Effect of solid state shear milling on structure and properties of poly (vinyl alcohol)/shell powder composite prepared by thermal processing. *Mater. Res. Express* **2019**, *6*, 065318.
(7) Yang, S. Y.; O'Cearbhaill, E. D.; Sisk, G. C.; Park, K. M.; Cho, W. K.; Villiger, M.; Bouma, B. E.; Pomahac, B.; Karp, J. M. A bio-inspired swellable microneedle adhesive for mechanical interlocking with tissue. *Nat. Commun.* **2013**, *4*, 1702.
(8) Yang, C.; Han, R.; Nie, M.; Wang, Q. Interfacial reinforcement mechanism in poly (lactic acid)/natural fiber biocomposites featuring ZnO nanowires at the interface. *Mater. Des.* **2020**, *186*, 108332.
(9) Moustafa, H.; Youssef, A. M.; Duquesne, S.; Darwish, N. A. Characterization of bio-filler derived from seashell wastes and its effect on the mechanical, thermal, and flame retardant properties of ABS composites. *Polym. Compos.* **2017**, *38*, 2788−2797.
(10) Li, Y.; Huang, P.; Guo, S.; Nie, M. A promising and green strategy for recycling waste oyster shell powder as bio-filler in polypropylene via mycelium-enlightened interfacial interlocking. *J. Cleaner Prod.* **2020**, *272*, 122694.
(11) Chong, M. H.; Chun, B. C.; Chung, Y. C.; Cho, B. G. Fire-retardant plastic material from oyster-shell powder and recycled polyethylene. *J. Appl. Polym. Sci.* **2006**, *99*, 1583−1589.
(12) Heriyanto; Pahlevani, F.; Sahajwalla, V. Effect of different waste filler and silane coupling agent on the mechanical properties of powder-resin composite. *J. Cleaner Prod.* **2019**, *224*, 940−956.
(13) Zou, M.; Wu, Y.; Redmile-Gordon, M.; Wang, D.; Liu, J.; Huang, Q.; Cai, P. Influence of surface coatings on the adhesion of Shewanella oneidensis MR-1 to hematite. *J. Colloid Interface Sci.* **2022**, *608*, 2955−2963.
(14) Zhang, H.; Liang, T.; Liu, Y.; Misra, R.; Zhao, Y. Low-surface-free-energy GO/FSiAC coating with self-healing function for anticorrosion and antifouling applications. *Surf. Coat. Technol.* **2021**, *425*, 127690.
(15) Zhang, K.; Li, X.; Nie, M.; Wang, Q. Helical flow-driven alignment of off-axial silver-functionalized titanium dioxide fibers in polypropylene tube suitable for medical applications. *Compos. Sci. Technol.* **2018**, *158*, 121−127.
(16) Deng, H.; Yang, Y.; Tang, X.; Li, Y.; He, F.; Zhang, Q.; Huang, Z.; Yang, Z.; Yang, W. Phase-change composites composed of silicone rubber and Pa@SiO2@PDA double-shelled microcapsules with low leakage rate and improved mechanical strength. *ACS Appl. Mater. Interfaces* **2021**, *13*, 39394−39403.
(17) Fu, Y.; Yang, L.; Zhang, J.; Hu, J.; Duan, G.; Liu, X.; Li, Y.; Gu, Z. Polydopamine antibacterial materials. *Mater. Horiz.* **2021**, *8*, 1618−1633.
(18) Stebbins, N. D.; Ouimet, M. A.; Uhrich, K. E. Antibiotic-containing polymers for localized, sustained drug delivery. *Adv. Drug Delivery Rev.* **2014**, *78*, 77−87.
(19) Fu, Y.; Liu, L.; Zhang, L.; Wang, W. Highly conductive one-dimensional nanofibers: silvered electrospun silica nanofibers via poly (dopamine) functionalization. *ACS Appl. Mater. Interfaces* **2014**, *6*, 5105−5112.
(20) Huang, Y.; Bai, L.; Yang, Y.; Yin, Z.; Guo, B. Biodegradable gelatin/silver nanoparticle composite cryogel with excellent anti-bacterial and antibiofilm activity and hemostasis for Pseudomonas aeruginosa-infected burn wound healing. *J. Colloid Interface Sci.* **2022**, *608*, 2278−2289.
(21) Liang, Y.; Liang, Y.; Zhang, H.; Guo, B. Antibacterial biomaterials for skin wound dressing. *Asian J. Pharm. Sci.* **2022**, *17*, 353−384.
(22) Lee, H.; Dellatore, S. M.; Miller, W. M.; Messersmith, P. B. Mussel-inspired surface chemistry for multifunctional coatings. *Science* **2007**, *318*, 426−430.
(23) Cheng, S.; Lau, K.-t.; Liu, T.; Zhao, Y.; Lam, P.-M.; Yin, Y. Mechanical and thermal properties of chicken feather fiber/PLA green composites. *Composites, Part B* **2009**, *40*, 650−654.
(24) Wu, Y.; Jia, W.; An, Q.; Liu, Y.; Chen, J.; Li, G. Multiaction antibacterial nanofibrous membranes fabricated by electrospinning: an excellent system for antibacterial applications. *Nanotechnology* **2009**, *20*, 245101.
(25) Ye, Q.; Zhou, F.; Liu, W. Bioinspired catecholic chemistry for surface modification. *Chem. Soc. Rev.* **2011**, *40*, 4244−4258.
(26) Bhuvaneswari, V.; Rajeshkumar, L.; Nimel Sworna Ross, K. Influence of bioceramic reinforcement on tribological behaviour of aluminium alloy metal matrix composites: experimental study and analysis. *J. Mater. Res. Technol.* **2021**, *15*, 2802−2819.
(27) Cabrera-Penna, M.; Rodríguez-Páez, J. Calcium oxyhydroxide (CaO/Ca (OH) 2) nanoparticles: Synthesis, characterization and evaluation of their capacity to degrade glyphosate-based herbicides (GBH). *Adv. Powder Technol.* **2021**, *32*, 237−253.
(28) Dang, Z.-M.; Yuan, J.-K.; Zha, J.-W.; Zhou, T.; Li, S.-T.; Hu, G.-H. Fundamentals, processes and applications of high-permittivity polymer−matrix composites. *Prog. Mater. Sci.* **2012**, *57*, 660−723.
(29) Qiang, F.; Wang, G.; Liu, C. Polyethylene toughened by CaCO3 particles: The interface behaviour and fracture mechanism in high density polyethylene/CaCO3 blends. *Polymer* **1995**, *36*, 2397−2401.
(30) Lee, H. A.; Park, E.; Lee, H. Polydopamine and its derivative surface chemistry in material science: a focused review for studies at KAIST. *Adv. Mater.* **2020**, *32*, 1907505.
(31) Liu, Y.; Yang, T.; Zhang, B.; Williams, T.; Lin, Y. T.; Li, L.; Zhou, Y.; Lu, W.; Kim, S. H.; Chen, L. Q.; et al. Structural insight in the interfacial effect in ferroelectric polymer nanocomposites. *Adv. Mater.* **2020**, *32*, 2005431.
(32) Yu, R.; Zhang, H.; Guo, B. Conductive biomaterials as bioactive wound dressing for wound healing and skin tissue engineering. *Nano-micro lett.* **2022**, *14*, 1.

https://doi.org/10.1021/acsomega.2c04779
ACS Omega 2022, 7, 36672−36678